



Spectroscopic and dielectric properties of crystallized PbO–Sb₂O₃–As₂O₃:NiO glass system

A. Padmanabham, Y. Gandhi, T. Satyanarayana, N. Veeraiah*

Department of Physics, Acharya Nagarjuna University-Nuzvid Campus, Nuzvid 521201, A.P., India

ARTICLE INFO

Article history:

Received 16 August 2009

Received in revised form 28 August 2009

Accepted 31 August 2009

Available online 8 September 2009

Keywords:

Dielectric response

Optical properties

X-ray diffraction

ABSTRACT

Glasses of the composition 40PbO–(20–*x*)Sb₂O₃–40As₂O₃ were crystallized with different concentrations of NiO (*x*) ranging from 0 to 1.5 mol%. The samples were characterized by X-ray diffraction, scanning electron microscopy and differential thermal analysis techniques. The X-ray diffraction and the scanning electron microscopic studies have revealed the presence of NiSb₂O₆, NiAs₂O₄, Ni₂As₂O₇, Pb₅Sb₂O₈, PbSb₂O₆, Pb₅Sb₄O₁₁ crystalline phases in these samples. Spectroscopic (IR and optical absorption), magnetic and dielectric studies have been investigated. The IR spectral studies have pointed out the glass ceramic network is composed of conventional AsO₃ and SbO₃ structural units; these studies have further indicated that the concentration of symmetrical vibrations of above structural groups decrease with increase in the concentration of NiO beyond 0.8 mol%. The analysis of the results of optical absorption, magnetic properties and dielectric properties has indicated that there is a gradual transformation of Ni²⁺ ions from octahedral to tetrahedral positions when the concentration of the crystallizing agent NiO is increased beyond 0.8 mol%. From these results it is also assessed that the glass crystallized with about 0.8 mol% of NiO is more suitable for getting maximum luminescence efficiency in the NIR region.

© 2009 Elsevier B.V. All rights reserved.

1. Introduction

Crystalline glass materials with appropriate transition metal ions like nickel as nucleating agents are considered as better candidates for ultra-broad band optical amplifiers that are widely used in telecommunication systems [1]; in the glass ceramic materials non-radiative losses over the relaxation of excited states of luminescence ions are relatively low when compared with glasses and crystalline materials. Though, the rare earth ions doped glasses and glass ceramics were considered as the suitable candidates for such applications, but the optical amplification bandwidth in these materials is narrowed, due to the fact that the emission bands of 4f–4f transition of the rare earth ions are very sharp. Additionally, if the care is taken to minimize the size of the micro-crystals (far less than the wavelength of interest) in the glass ceramics during the synthesis, the light scattering caused by these crystals is negligibly low and thereby a substantial improvement in the quantum efficiency of the broad band emission can be achieved. Further, the lasing ions disperse more evenly in crystalline embryos of bulk glass ceramic samples when compared with as quenched glass samples.

Among various transition metal ions, Cr⁴⁺ ions were considered as potential candidates for high gain optical amplifiers with

larger bandwidths in glass ceramics; nevertheless, the chromium ions exist in multi-valent states, viz., Cr³⁺, Cr⁴⁺, Cr⁵⁺ and Cr⁶⁺ [2,3]. The same is true in case of other transition metal ions like Ti and Mn [4,5]. Hence, it is too difficult to have the strict control over the required or suitable valence state of these ions embedded in crystal phases. Unlike these ions, the nickel ions mostly exist in divalent state and are extremely stable and no special care is necessary during synthesis to retain nickel ions in divalent state. There have been hardly any reports so far about reduction or oxidation of Ni²⁺ ions into lower or higher oxidation states, respectively in glasses or glass ceramic matrices during synthesis. Further, Ni²⁺ is an ion with exceptionally large crystal stabilization energies particularly when it is in octahedral field [6]. Ni²⁺ ions exhibit several strong absorption bands in the visible and NIR regions where the pumping sources are easily available. The octahedrally positioned Ni²⁺ ions in glass network are expected to exhibit eye safe laser emission of wavelength of about 1.5 μm due to ³T₂ → ³A₂ transition, even at room temperature, which is of great importance in telecommunications [7]. There have been considerable recent studies on lasing action and other physical properties of nickel ions in various glass and glass ceramic materials [8–11].

The heavy metal oxide based glass ceramics like lead antimony oxide based glass ceramics possess high refractive index and are transparent to far infrared wavelengths [12–14]; these materials have got potential applications in non-linear optical devices (such as ultrafast optical switches, power limiters and broad band optical amplifiers operating around 1.5 μm) [15,16]. Further, antimony

* Corresponding author. Tel.: +91 9440015188; fax: +91 8656235551.
E-mail address: nvr8@rediffmail.com (N. Veeraiah).

Table 1The physical properties of PbO–Sb₂O₃–As₂O₃:NiO glass ceramics (densities of pre-crystallized samples are shown in brackets).

Glass ceramic	N ₀	N ₂	N ₄	N ₆	N ₈	N ₁₀	N ₁₅
Density <i>d</i> (gm/cm ³)	5.790 (5.735)	5.757 (5.738)	5.752 (5.741)	5.747 (5.744)	5.740 (5.737)	5.743 (5.740)	5.764 (5.757)
Average molecular weight \bar{M}	226.716	226.282	225.848	225.415	224.981	224.547	223.463
Ni ²⁺ ion concentration N _i (10 ²² ions/cm ³)	–	0.306	0.614	0.921	1.227	1.541	2.330
Inter-ionic distance of nickel ions <i>r</i> _i (Å)	–	6.88	5.46	4.77	4.34	4.02	3.50
Polaron radius <i>r</i> _p (Å)	–	2.77	2.20	1.92	1.75	1.62	1.41

oxide participates in the glass network with SbO₃ structural units and can be viewed as tetrahedrons with the oxygen situated at three corners and the lone pair of electrons of antimony (Sb³⁺) at the fourth corner localized in the third equatorial direction of Sb atom. The deformability of this pair probably could make these glass ceramics to exhibit non-linear optical susceptibility described by third rank polar tensors. Antimony ions may also exist in Sb⁵⁺ state, participate in the formation of glass network with Sb⁵⁺O₄ structural units. Recently we have reported the non-linear optical (NLO) effects of antimony oxide based glass ceramics; these studies have yielded valuable information regarding the suitability of these materials for NLO devices [17,18]. The addition of As₂O₃ to PbO–Sb₂O₃ glasses may improve the glass forming ability (since Sb₂O₃ is a conditional glass former). As₂O₃ is the only strong network former besides GeO₂ that exhibit significant transmission potential farther into the infrared. This is illustrated by calculated wavelength of λ_0 , the material dispersion crossover point which is 1.3 μ m for P₂O₅, B₂O₃ and SiO₂, 1.7 μ m for GeO₂ and 1.9 μ m for As₂O₃ [19,20]. Thus PbO–Sb₂O₃–As₂O₃ glass network provides a highly suitable environment for Ni²⁺ ions to exhibit emission in NIR regions.

The present work is devoted to report a variety of physical properties that include dielectric studies, spectroscopic studies (IR, optical absorption) of crystallized PbO–Sb₂O₃–As₂O₃ glasses with varying concentrations of NiO as nucleant. The crystallization behavior and microstructure of glass ceramic products produced have also been investigated by means of XRD, SEM, DTA and EDS. The study is also intended to comment on the suitability of these glass ceramic materials for laser emission in NIR region.

2. Experimental

Within the possible glass forming region of PbO–Sb₂O₃–As₂O₃ system, a particular compositions 40PbO–(20–*x*)Sb₂O₃–40As₂O₃:*x*NiO with the value of *x* ranging from 0 to 1.5 mol% is chosen for the present study; the samples are labeled as N₀ (*x*=0), N₂ (*x*=0.2), N₄ (*x*=0.4), N₆ (*x*=0.6), N₈ (*x*=0.8), N₁₀ (*x*=1.0), N₁₅ (*x*=1.5). Analytical grade reagents of Sb₂O₃, As₂O₃, PbO and NiO powders in appropriate amounts (all in mol%) were thoroughly mixed in an agate mortar and melted in a platinum crucible in the temperature range of 600–650 °C in a PID temperature controlled furnace for about 1 h. The resultant bubble free melt was then poured in a brass mould and subsequently annealed at 200 °C. The glass specimens with various concentrations of NiO were heat treated in a furnace at 300 °C for 6 h. Automatic controlling furnace was used to keep the temperature at the desired level. After the heat treatment in the furnace at specified temperature, the samples were chilled in air to room temperature. The samples prepared were ground and optical polished to the dimensions of 1 cm × 1 cm × 0.2 cm. It may be noted here that as the concentration of NiO is increased, the colour of the glass ceramics is gradually turned from brown to thick brown and beyond 1.5 mol% of NiO, the colour of the samples became thick black and opaque. Hence, the concentration of the dopant is limited to only up to 1.5 mol%. The crystalline phases in the glass ceramic samples were identified by recording XRD spectra using Rigaku D/Max ULTIMA III X-ray diffractometer with CuK_α radiation. Scanning electron microscopy studies were also carried out on these samples to observe the crystallinity using HITACHI S-3400N Scanning Electron Microscope. Differential thermal analysis of these samples were carried out using Mettler Toledo, TGA/SDTA85/° instrument with a programmed heating rate of 10 °C/min, in the temperature range of 30–750 °C. The density of the glass ceramics was determined to an accuracy of (±0.0001) by the standard principle of Archimedes' with *o*-xylene (99.99% pure) as the buoyant liquid using Ohaus digital balance Model AR2140. Infrared transmission spectra were recorded on a JASCO-FT/IR-5300 spectrophotometer up to a resolution of 0.1 cm⁻¹ in the spectral range 400–1200 cm⁻¹ using potassium bromide pellets (300 mg) containing pulverized sample (1.5 mg). These pellets were pressed in a vacuum die at ~680 MPa. The optical absorption spectra of

the glass ceramics were recorded with a spectral resolution of 0.1 at room temperature in the spectral wavelength range covering 300–1500 nm using JASCO Model V-670 UV–vis–NIR spectrophotometer. The details of measurements of dielectrics were just similar to those reported in our earlier papers [21–23].

3. Results

The gradual increase of the content of nucleating agent NiO in the glass matrix, caused a slight increase in the density of these materials (Table 1). However, the values of density are always found to be higher than those of corresponding amorphous materials. From the measured values of the density and average molecular

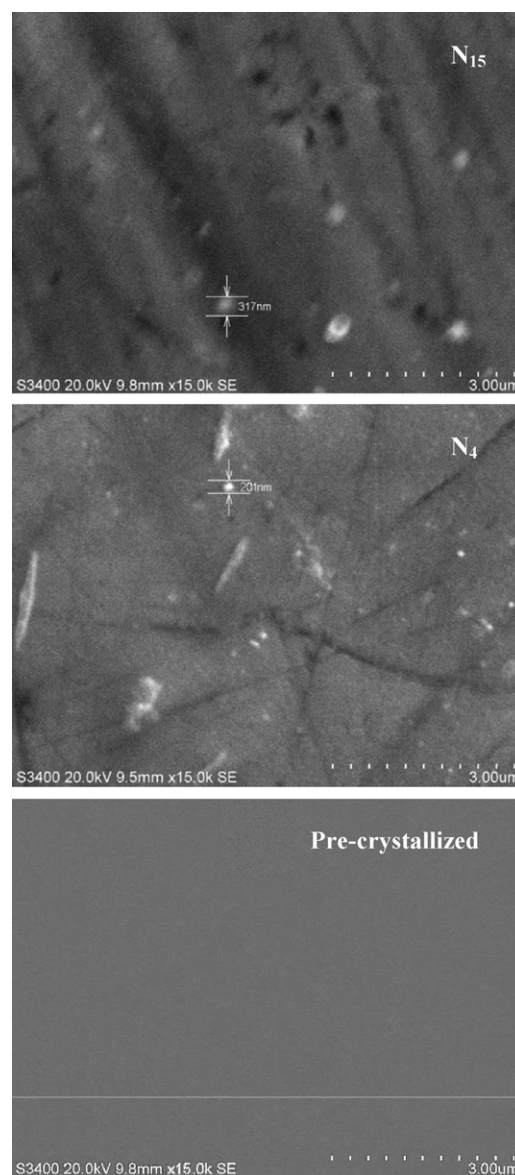


Fig. 1. SEM images for some of PbO–Sb₂O₃–As₂O₃:NiO samples.

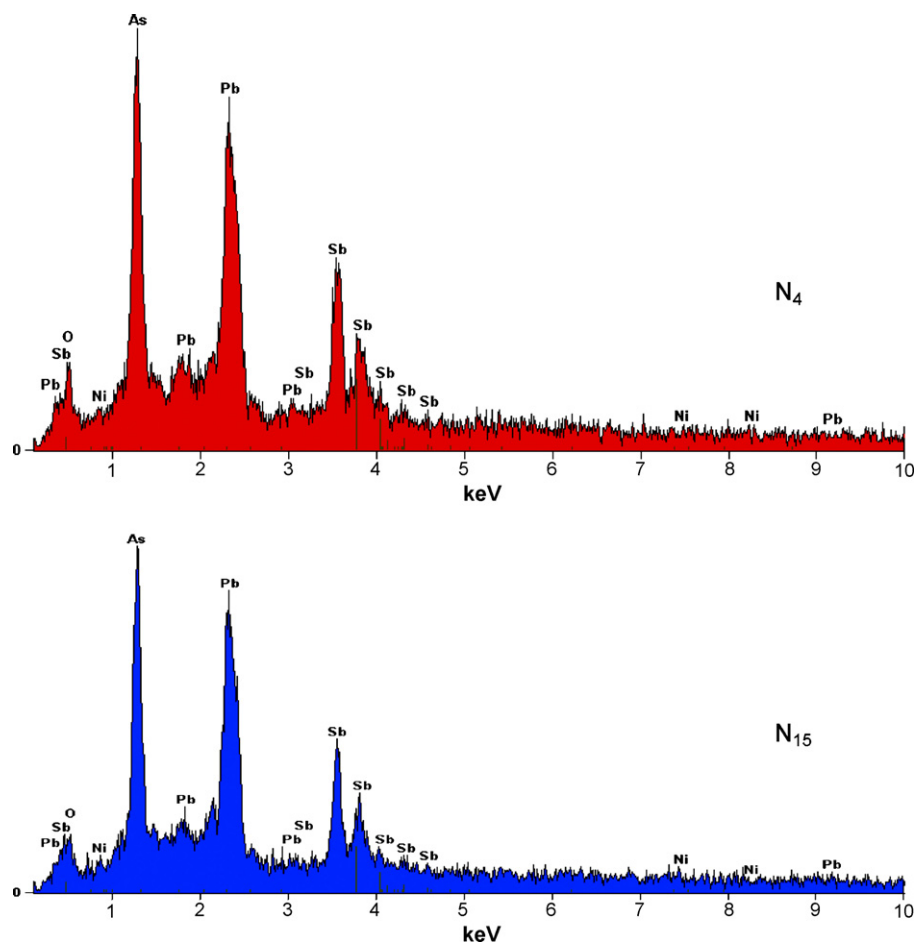


Fig. 2. EDS traces for some of the PbO–Sb₂O₃–As₂O₃:NiO glass ceramic samples.

weight \bar{M} of the samples, various other physical parameters such as nickel ion concentration N_i , mean nickel ion separation r_i , polaron radius r_p in PbO–Sb₂O₃–As₂O₃:NiO glass ceramic samples are computed and presented in Table 1.

The prepared PbO–Sb₂O₃–As₂O₃:NiO glass ceramic samples contain well-defined, randomly distributed crystals entrenched in glassy matrix with an average diameter of 200–300 nm. The residual glass phase is acting as interconnecting zones among the crystallized areas making the samples free of voids and cracks; this can be visualized clearly from the scanning microscopy pictures of the (Fig. 1) samples. Thus, from these pictures it can also be concluded that NiO, enhanced the phase separation tendency of various crystalline phases; this fact reflects specific overlap integral between the 3d levels of Ni ion and the delocalized anti-bonding p-states of antimony. The chemical makeup of the crystal phases is characterized using EDS (Fig. 2); the analysis indicated the presence of lead, arsenate, antimony, nickel and oxygen elements in the samples. X-ray diffraction studies (Fig. 3) indicate the forma-

tion of NiSb₂O₆, NiAs₂O₄, Ni₂As₂O₇, Pb₅Sb₂O₈, PbSb₂O₆, Pb₅Sb₄O₁₁ (JCPDS card numbers 38-1083, 44-0438, 10-0326, 22-0381, 34-0912 and 21-0941, respectively [24]) crystalline phases that are kinetically and thermodynamically feasible seemed to be products in these samples. The Ni rich areas in the samples may enhance the reactivity of Ni ion with the other oxides that precipitate as a high density of fine Ni rich crystals. These tiny crystals act as heterogeneous nuclei for the crystallization of the remaining glass. The diffraction data also indicate that, in these samples, the antimony ions exist in Sb⁵⁺ state in addition to Sb³⁺ state; however, the concentration of Sb³⁺ ions seems to be dominant over Sb⁵⁺ ions in the samples crystallized with lower concentrations of NiO.

In Fig. 4, we have shown differential thermal analysis traces (DTA) for some of the PbO–Sb₂O₃–As₂O₃:NiO glass ceramics in the temperature region 30–750 °C. All DTA traces indicate typical glass transitions with the inflection point between 240 and 290 °C. The glass transitions temperature shows slightly increasing trend with increase in the content of nucleating agent (Table 2). The endothermic effect is followed by well-defined exothermic effects at the two steps of crystallization temperatures. Another endothermic peak in the region of 500–640 °C, due to the re-melting of the samples is also observed in these traces.

The optical absorption edge observed at 380 nm for glass N₂ is found to be shifted to higher wavelength with increase in the concentration of NiO up to 0.8 mol%; beyond this concentration the edge is observed to shift towards lower wavelength (Fig. 5). From the observed absorption edges, we have evaluated the optical band gaps (E_0) of these samples by drawing Urbach plots (Fig. 6) between $(\alpha h\nu)^{1/2}$ and $h\nu$. The value of the optical band gap exhib-

Table 2
Summary of the data on differential thermal analysis studies of PbO–Sb₂O₃–As₂O₃:NiO glass ceramics.

Glass	T_g (°C)	T_c (°C)	T_m (°C)
N ₂	242	378	568
N ₄	244	377	572
N ₆	247	378	576
N ₈	249	365	584
N ₁₀	260	392	590
N ₁₅	271	405	603

Table 3
Summary of data on optical absorption spectra of PbO–Sb₂O₃–As₂O₃:NiO glass ceramics.

Transition of nickel ions	Band positions in nm					
	N ₂	N ₄	N ₆	N ₈	N ₁₀	N ₁₅
Octahedral transitions (nm)						
³ A ₂ (F) → ³ T ₂ (F)	1274	1278	1279	1283	1281	1280
³ A ₂ (F) → ³ T ₁ (F)	792	793	794	797	796	795
³ A ₂ (F) → ¹ T ₂ (D)	471	476	477	483	480	478
Tetrahedral transitions (nm)						
³ A ₂ (F) → ³ T ₁ (P)	595	593	591	585	587	589
Cutoff wavelength (nm)	380	384	386	391	389	387
Optical band gap E _o (eV)	3.18	3.165	3.14	3.09	3.10	3.12
Dq (cm ⁻¹)	784.9	782.5	781.9	779.4	780.6	781.3
B (cm ⁻¹)	733.0	735.2	743.2	750.8	738.0	732.3
Nephelauxetic ratio	0.681	0.683	0.690	0.697	0.685	0.680

Table 4
Summary of data on magnetic properties of PbO–Sb₂O₃–As₂O₃:NiO glass ceramics.

Glass ceramic	Conc. NiO (mol%)	Magnetic susceptibility χ (10 ⁻⁵ emu)	μ _{eff} (μ _B)
N ₂	0.2	1.89	3.00
N ₄	0.4	4.04	3.10
N ₆	0.6	6.63	3.24
N ₈	0.8	9.27	3.33
N ₁₀	1.0	16.1	3.90
N ₁₅	1.5	26.2	4.05

ited a decreasing trend up to 0.8 mol% of NiO and beyond that is found to increase.

Additionally, the spectrum of the sample (N₂) exhibited, four clearly resolved absorption bands in the visible and NIR regions at 1274 nm (O_{h1}), 792 nm (O_{h2}) and 471 nm (O_{h3}) and 595 nm (tetrahedral band). As the concentration of NiO is increased up to 0.8 mol%, the intensity of the octahedral bands (O_h bands) is observed to increase with a shift towards slightly higher wavelength; in this concentration range the intensity of the tetrahedral

band (T_d band) is observed to decrease with a slight shift towards higher wavelengths. With the raise of NiO content from 0.8 to 1.5 mol%, the tetrahedral band is observed to grow at the expense of octahedral bands. The summary of the data on optical absorption spectra of these glasses is furnished in Table 3.

Magnetic susceptibility of PbO–Sb₂O₃–As₂O₃:NiO glass ceramics measured at room temperature is observed to increase gradually with increase in the content of crystallizing agent NiO. From the values of magnetic susceptibilities, the magnetic moment of Ni²⁺ ion is evaluated and presented in Table 4.

In the infrared spectrum (Fig. 7) of glass ceramic sample N₂, the band due to ν₁ vibrations of SbO₃ structural groups is observed at about 943 cm⁻¹ and the band related to ν₂ vibrations of these units is observed at 621 cm⁻¹. The IR spectrum of crystalline As₂O₃ is expected to exhibit four fundamental absorption bands at ν₁ (1050 cm⁻¹), ν₂ (618 cm⁻¹), ν₃ (795 cm⁻¹) and ν₄ (505 cm⁻¹) [20]. In the spectrum of glass ceramic N₂, the ν₁ band is appeared at 1040 cm⁻¹, whereas, the ν₂ bands and the ν₃ bands of SbO₃ and AsO₃ structural groups are merged and exhibited common meta-centers at 621 and 762 cm⁻¹, respectively. In the region of ν₄

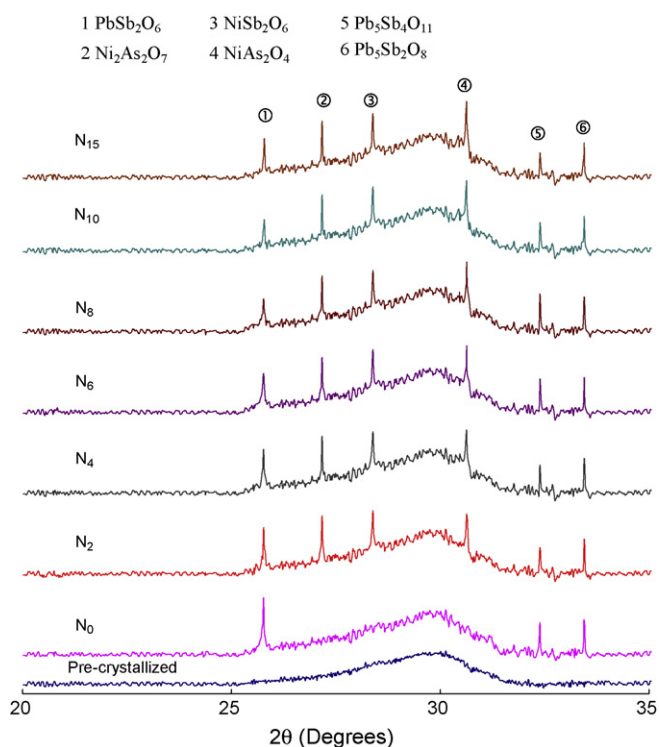
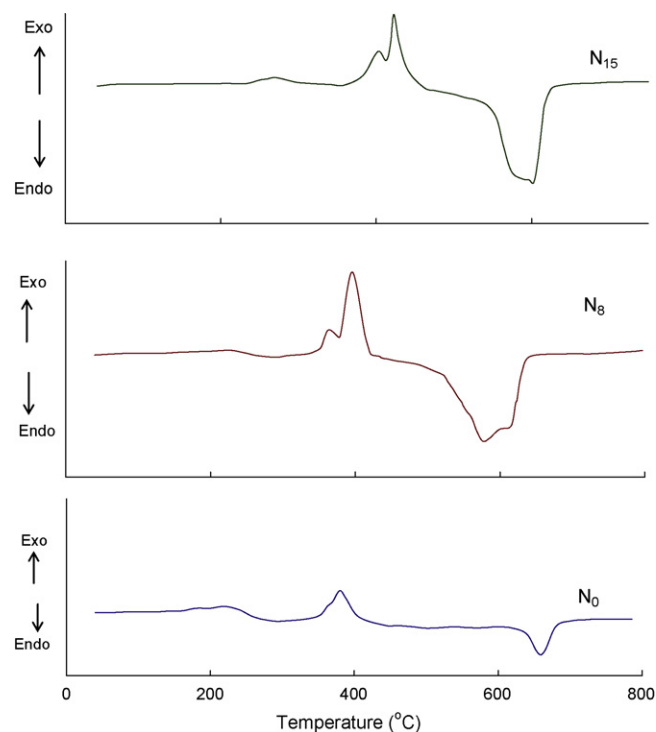
**Fig. 3.** XRD patterns of PbO–Sb₂O₃–As₂O₃ glasses crystallized with different concentrations of NiO.**Fig. 4.** Differential thermal analysis traces (DTA) for some of the PbO–Sb₂O₃–As₂O₃:NiO glass ceramics.

Table 5

Summary of the data on the positions of the bands in IR spectra of PbO–Sb₂O₃–As₂O₃:NiO glass ceramics.

Glass ceramic	ν_1 (cm ⁻¹)		As ₂ O ₃ /Sb ₂ O ₃ (cm ⁻¹)		PbO ₄ (cm ⁻¹)
	As ₂ O ₃	Sb ₂ O ₃	ν_3	ν_2	
N ₂	1023	943	621	762	470
N ₄	1027	947	622	768	470
N ₆	1039	951	624	774	470
N ₈	1061	958	633	781	470
N ₁₀	1052	954	631	778	470
N ₁₅	1043	949	627	775	470

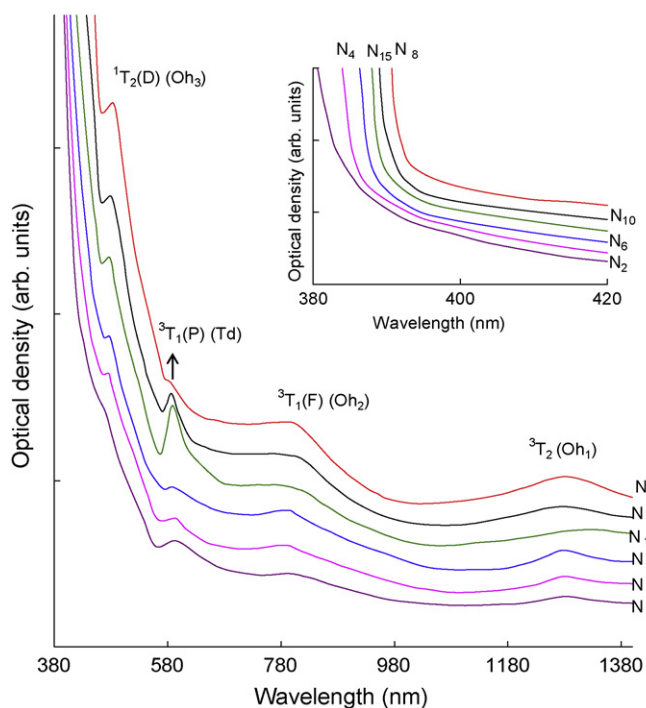


Fig. 5. Optical absorption spectra of PbO–Sb₂O₃–As₂O₃:NiO glass ceramics. Inset represents the absorption near the cutoff wavelength.

vibrations of AsO₃ structural units, it is quite likely that the vibrations due to PbO₄ structural groups could be present; in fact the vibrational band due to PbO₄ units was reported at 470 cm⁻¹ in a number of other glass systems [25]. The summary of IR spectra of these samples is shown in Table 5. As the content of the crystallizing agent NiO is increased gradually up to 0.8 mol%, the intensity of bands due to symmetric stretching and symmetric bending vibrations of SbO₃ and AsO₃ structural groups is also observed to decrease; for further increase of NiO content these bands have exhibited a reversal trend.

The dielectric constant ϵ' and loss $\tan \delta$ at room temperature ($\approx 30^\circ\text{C}$) of PbO–Sb₂O₃–As₂O₃ glass crystallized with 0.2 mol% of

Table 6

Data on dielectric loss of PbO–Sb₂O₃–As₂O₃:NiO glass ceramics.

Glass ceramic	(Tan δ) _{Max.Avg}	Temp. region of relaxation ($^\circ\text{C}$)	A.E. for dipoles (eV)
N ₂	0.0222	100–140	3.65
N ₄	0.0236	90–132	3.53
N ₆	0.0251	85–128	3.15
N ₈	0.0300	70–115	2.84
N ₁₀	0.0282	76–112	2.97
N ₁₅	0.0268	80–115	3.03

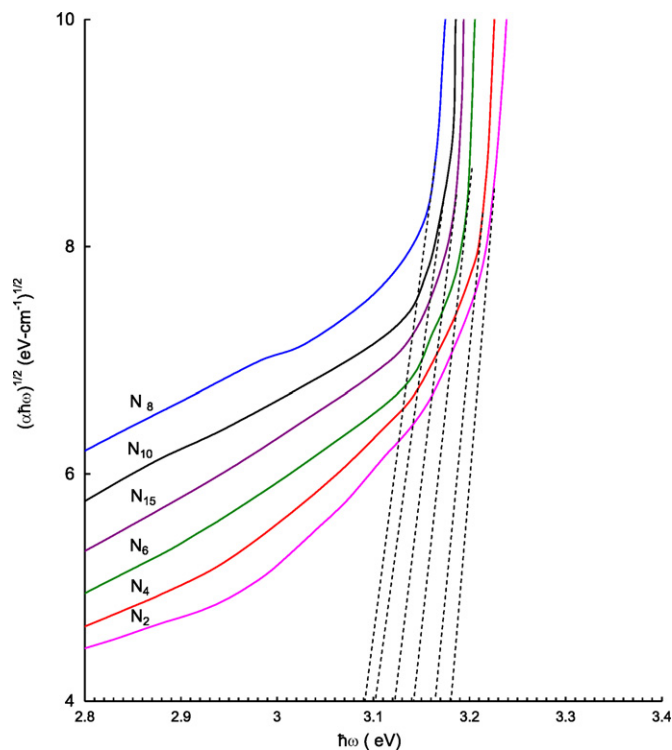


Fig. 6. Plots to evaluate optical band gaps for PbO–Sb₂O₃–As₂O₃:NiO glass ceramics.

NiO at 100 kHz are measured to be 11.5 and 0.011, respectively; these values found to increase considerably with decrease in frequency. Fig. 8 represents the variation of dielectric constant and loss with frequency at room temperature of PbO–Sb₂O₃–As₂O₃ glasses crystallized with different concentrations of NiO; the parameters, ϵ' and $\tan \delta$ are observed to increase with the concentration of NiO up to 0.8 mol% at any frequency.

The temperature dependence of ϵ' at 1 kHz of PbO–Sb₂O₃–As₂O₃ glasses crystallized with different concentrations of NiO is shown in Fig. 9 and at different frequencies of glass ceramic sample N₈ is shown as the inset. The value of ϵ' is found to exhibit a considerable increase at higher temperatures especially at lower frequencies; however the rate of increase of ϵ' with temperature is found to be the maximum for the sample N₈.

A comparison plot of variation of $\tan \delta$ with temperature, measured at a frequency of 10 kHz for all the glass ceramic samples is presented in Fig. 10. The inset (a) of this figure represents the temperature dependence of $\tan \delta$ of sample N₁₀ at different frequencies. The dependence of dielectric loss with temperature at different frequencies exhibits distinct maxima indicating dipolar relaxation character of dielectric loss in these glass ceramic samples. From these curves, it is also observed that the region of relaxation shifts towards lower temperatures (with broadening of relaxation peaks and increasing value of $(\tan \delta)_{\text{max}}$) with increase in the concentration of the nucleating agent up to 0.8 mol%. The effective activation energy W_d for the dipoles is evaluated for all the glass ceramic samples using the relation:

$$f = f_0 e^{-W_d/kT} \quad (1)$$

and its variation with the concentration of NiO is shown as inset (b) of Fig. 10; the activation energy is found to be minimum for the sample N₈. The pertinent data related to dielectric loss of these glasses are presented in Table 6.

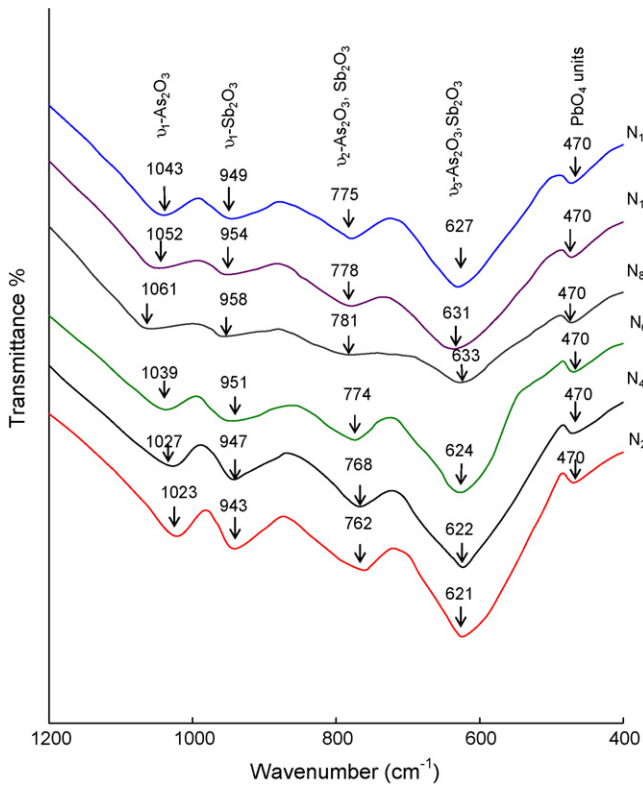


Fig. 7. IR spectra of PbO-Sb₂O₃-As₂O₃:NiO glass ceramics.

The a.c. conductivity σ_{ac} is calculated at different temperatures, using the relation:

$$\sigma_{ac} = \omega \epsilon_0 \epsilon' \tan \delta \quad (2)$$

for different frequencies and the plots of $\log \sigma_{ac}$ against $1/T$ are shown in Fig. 11 for all the glass ceramics at 100 kHz. From these plots, the activation energy for conduction in the high temperature region over which a near linear dependence of $\log \sigma_{ac}$ with $1/T$ could be observed is evaluated and presented in Table 7; this activation energy is also found to decrease gradually with increase in the concentration of the crystallizing agent up to 0.8 mol% (inset (a) of Fig. 11).

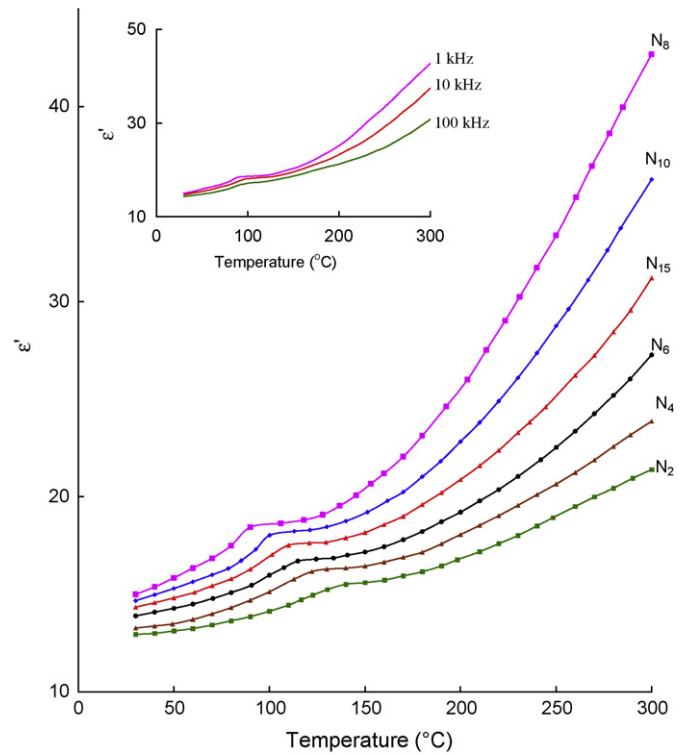


Fig. 9. A comparison plot of variation of dielectric constant with temperature at 1 kHz for PbO-Sb₂O₃-As₂O₃:NiO glass ceramics. Inset gives the variation of dielectric constant with temperature at different frequencies of glass ceramic N₈.

4. Discussion

In PbO-Sb₂O₃-As₂O₃:NiO glass system, Sb₂O₃ is an incipient glass network former and as such does not readily form the glass but does so in the presence of the modifier oxides like PbO and the strong glass former As₂O₃. Antimony oxide participates in the glass network with SbO₃ structural units with the oxygen at three corners and the lone pair of electrons of antimony at the fourth corner as mentioned earlier. In the glass network, normally the Sb-O distances lie in between 2.0 and 2.6 Å [26–28]. The coordination polyhedra are joined by sharing the corners to form double infinite chains with the lone pairs pointing out from the chains. X-ray

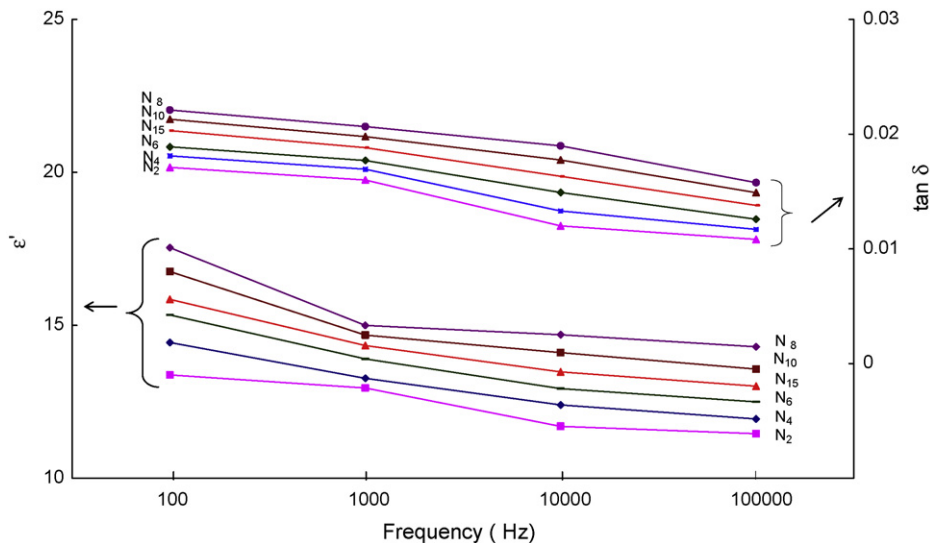


Fig. 8. Variation of dielectric constant and loss with frequency of PbO-Sb₂O₃-As₂O₃:NiO samples measured at room temperature.

Table 7
Summary of data on ac conductivity of PbO–Sb₂O₃–As₂O₃:NiO glass ceramics.

Glass ceramic	$N(E_F)$ in (10^{20} , $\text{eV}^{-1} \text{cm}^{-3}$)	A.E. for conduction (eV)
N ₂	1.960	0.36
N ₄	2.105	0.33
N ₆	2.288	0.30
N ₈	2.778	0.23
N ₁₀	2.622	0.26
N ₁₅	2.452	0.28

diffraction studies have indicated that antimony ions also exist in Sb⁵⁺ state in these glass ceramics. As a participant of glass network, the local structure of Sb³⁺ cations become less symmetric and the strain energy in the glass network increases as a whole, thus resulting in a decrease in the additional activation energy that is necessary for glass network rearrangement. As a result we expect that more degree of disorder in glass ceramics containing Sb³⁺ ions rather than in the glass ceramics containing Sb⁵⁺ ions. Sb⁵⁺ ion participates in the glass network with Sb^VO₄ structural units as reported earlier [17].

As₂O₃ is a strong network former with corner sharing AsO₃ pyramidal units [29,30]. Further, there is a possibility for the cross-linking of a part of SbO₃ units with As³⁺ ions to form Sb–O–As bonds in the glass network. The presence of common meta-centers units of ν_2 and ν_3 vibrational bands in the ranges of SbO₃ and AsO₃ structural units, in the IR spectra of the glass ceramics in fact supports such a view point. However, earlier EXAFS studies indicated that Sb^VO₄ units are more compatible in the network forming rather than SbO₃ trigonal pyramids units to form linkages with the conventional AsO₃ structural units [31]. The reasons are obvious; Sb³⁺ ion with its lone electron pair occupies a greater angular volume than a bonding pair of electrons. As a participant of glass network, the local structure of Sb³⁺ cations become less symmetric and the strain energy in the glass network increases as a whole,

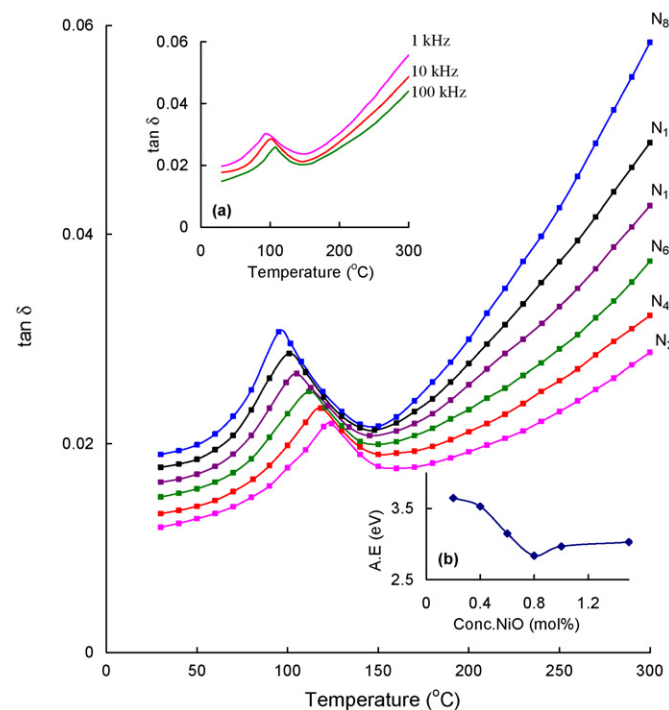


Fig. 10. A comparison plot of variation of dielectric loss with temperature at 10 kHz for PbO–Sb₂O₃–As₂O₃:NiO glass ceramics. Inset (a) gives the variation of dielectric loss with temperature at different frequencies of glass ceramic N₁₀ and inset (b) shows the variation of activation energy for dipoles with the concentration of nucleating agent.

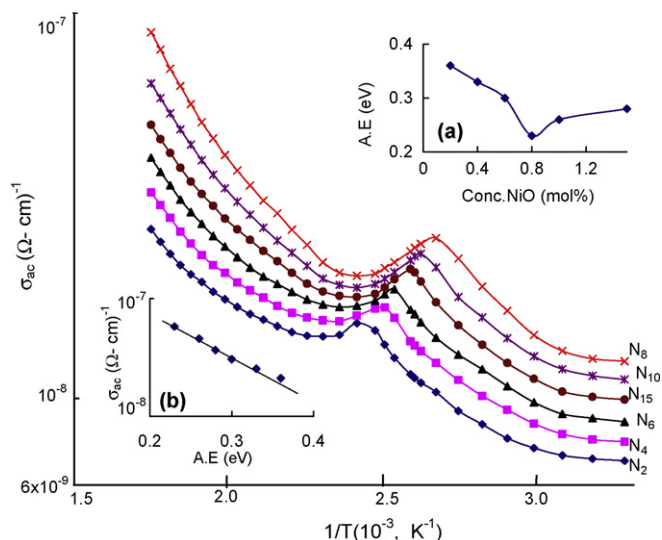


Fig. 11. Variation of σ_{ac} with $1/T$ at 100 kHz of PbO–Sb₂O₃–As₂O₃:NiO glass ceramic. Inset (a) represents the variation of activation energy for conduction with NiO concentration. Inset (b) shows the variation of $\log \sigma (\omega)$ vs. activation energy for conduction.

thus resulting in a decrease in the additional activation energy that is necessary for glass network rearrangement. As a result we expect that more degree of disorder in glasses containing Sb³⁺ ions rather than in the glasses containing Sb⁵⁺ ions.

In general, the degree of structural compactness, the modification of the geometrical configuration of the glassy network, the size of the micro-crystals formed, change in the coordination of the glass forming ions and the fluctuations in the dimensions of the interstitial holes are the some of the factors that influence the density of the glass ceramic material. In the present case, progressive introduction of crystallizing agent NiO up to 0.8 mol% caused a considerable decrease in the density; this is an indicative of decreasing structural compactness of the material. The higher values of density observed for the sample N₁₅ indicates higher compactness for this sample.

The formation of NiSb₂O₆, NiAs₂O₄, Ni₂As₂O₇, Pb₅Sb₂O₈, PbSb₂O₆, Pb₅Sb₄O₁₁ crystalline phases detected from the XRD studies indicate the presence of NiSb₂O₆, PbSb₂O₆ phases clearly confirms the conversion of a fraction of Sb³⁺ ions into Sb⁵⁺ state in these glass ceramics. The relative variation in the intensity of the diffraction patterns also indicates the presence of higher concentration Sb⁵⁺ in the samples N₁₀ and N₁₅. The presence of different crystalline phases in these samples can also be visualized from scanning electron microscope pictures. The residual glass phase may act as interconnecting zones among the crystallized areas making the samples free of voids and cracks.

The appearance of different crystallization temperatures in the differential thermal analysis patterns of the glass ceramic samples obviously suggests the presence of different phases of crystallization in the samples. The analysis of the results of DTA studies indicates that with increase in the concentration of crystallizing agent NiO (beyond 0.8 mol%), there is a considerable increase in the glass transition temperature T_g . The higher augmented cross-link density of various structural groups and the increment in the closeness of packing are responsible for such increase of this parameter. These results apparently suggest that there is a growing presence of tetrahedrally positioned nickel ions which increase the cross-link density and decrease the mean bond strength. The appearance of different crystallization temperatures in the DTA pattern obviously suggests the presence of different phases of crystallization in the samples. The low degree of resolution of exothermic peaks of

the samples indicates overlapping of these peaks due to different crystalline phases.

The general shape of the crystallization peaks is strongly dependent with the nature of crystallization (bulk or surface) in the sample. For the surface crystallization we expect relatively wider peaks when compared with the peaks due to bulk crystallization [32]. The close examination of pattern of the DTA peaks reveals the enthalpy associated with the crystallization effect relatively small for the samples N₁₀ and N₁₅ indicating bulk crystallization prevails in these samples when compared with the rest of the samples.

Using Tanabe-Sugano diagrams for d⁸ ion, the observed octahedral bands in the optical absorption spectra are assigned to ³A₂(F) → ³T₂(F) (Oh₁), ³T₁(F) (Oh₂), ¹T₂(D) (Oh₃). Out of these, ³A₂(F) → ¹T₂(D) is attributed to spin forbidden octahedral band [33]. The band observed at about 595 nm is attributed to ³A₂(F) → ³T₁(P) tetrahedral transition [34]. The ligand field parameters Dq (crystal field splitting energy) and B (Racah parameter) are evaluated using energies of these transitions and the values obtained are furnished in Table 3. The observed enhancement of the absorption in the octahedral bands with increase in the content of NiO up to 0.8 mol% suggests the increasing presence of octahedrally positioned nickel ions and the increasing trend of tetrahedral band beyond 0.8 mol% of NiO indicates that the nickel ions prefer tetrahedral positions in this concentration range.

Further, the nephelauxetic ratio (β) evaluated from the Racah parameter (B), shows a decreasing trend; such a trend clearly suggests the decrease of the covalency around Ni²⁺ as the concentration of the nucleating agent is increased up to 0.8 mol%. The increasing trend of these values beyond 0.8 mol% of nucleating agent, indicates the increasing covalency environment for Ni²⁺ ions in the glass ceramic network. In the spectra, we have also observed the shifting of the octahedral bands towards higher wavelengths as the concentration of NiO is increased up to 0.8 mol%; such shift in the position of the bands indicates an increase in average distance of Ni–O.

The observed decrease in the optical band gap with the increase in the concentration of the nucleating agent may be understood as follows: the gradual increase in the concentration of octahedrally positioned Ni²⁺ ions, causes a creation of large number of donor centers; subsequently, the excited states of localized electrons originally trapped on Ni²⁺ sites begin to overlap with the unfilled 3d states on the neighboring impurity sites. As a result, the impurity band becomes more extended into the main band gap. This development might have shifted the absorption edge to the lower energy (Table 3) which leads up to a significant shrinkage in the band gap from the sample N₂ to N₈.

The magnetic properties of PbO–Sb₂O₃–As₂O₃:NiO glass ceramic samples arise from the paramagnetic Ni²⁺ (both tetrahedral and octahedral) ions. Magnetically, the octahedral Ni²⁺ complexes have relatively simple behavior and their magnetic moments are expected to lie in the range 2.9–3.4 μ_B [35] depending on the magnitude of the orbital contribution. Since, the ground state ³T₁(F) of tetrahedral Ni²⁺ ions possess much inherent orbital angular momentum, the magnetic moment of perfect tetrahedral Ni²⁺ should be $\sim 4.2\mu_B$. Even a slight distortion reduces this value markedly because of the orbital degeneracy. The fairly regular tetrahedral complexes of these ions are expected to have the magnetic moment in the range 3.5–4.1 μ_B [35]. The gradual increase of the effective magnetic moment from 3.33 μ_B (for sample N₈) to 4.05 μ_B (for sample N₁₅) confirms that there is a gradual transformation of the positions of Ni²⁺ ions from the octahedral sites to the tetrahedral sites as the concentration of crystallizing agent NiO is increased beyond 0.8 mol%.

The decrease in the intensity of the bands due to symmetric stretching and bending vibrations of AsO₃ and SbO₃ structural units in the IR spectra with increase in the concentration of the crys-

tallizing agent NiO up to 0.8 mol%, clearly suggests an increasing modifying action of these ions. It may be noted here that it is the octahedral ion that induce more non-bridging oxygens and structural disorder in the glass network. Hence, the analysis of IR spectral studies of the samples points out that there is a gradual transformation of nickel ions from octahedral to tetrahedral positions as the concentration of NiO is increased beyond 0.8 mol%.

The values of dielectric parameters viz., ϵ' , $\tan \delta$ and σ_{ac} at any frequency are found to increase with temperature and activation energy for a.c. conduction is observed to decrease with increase in the content of nucleating agent NiO up to 0.8 mol%; this is an indication of an increase in the space charge polarization. Such increase indicates the increasing concentration of Ni²⁺ ions that act as modifier in these samples. These modifying ions as mentioned earlier, generate bonding defects in the glass network. The defects thus produced create easy pathways for the migration of charges that would build up space charge polarization and facilitate to an increase in the dielectric parameters as observed [36,37].

We have obtained the increase in the value of $(\tan \delta)_{max}$ and decrease of the effective activation energy associated with the dipoles with increase in the content of NiO (up to 0.8 mol%) in the glass ceramic network (Table 6), these observations suggest an increasing freedom for dipoles to orient in the field direction, obviously due to increasing degree of disorder in glass ceramic network. The observed dielectric relaxation effects in PbO–Sb₂O₃–As₂O₃ glasses crystallized with different concentrations of NiO may be attributed to the association of octahedrally positioned Ni²⁺ ions with a pair of cationic vacancies as observed in a number of conventional glasses, glass ceramics and crystals that contain divalent positive ions as reported before [38].

The variation of $\log \sigma(\omega)$ vs. activation energy for conduction (in the high temperature region) is shown as inset (b) in Fig. 11; the graph yields a near straight line. This observation suggests that the conductivity enhancement is directly related to the thermally stimulated mobility of the charge carriers in the high temperature region. The progressive increase of conductivity with the increase of nickel content in the glass ceramic is a manifestation of the increasing concentration of mobile electrons, or polarons, involved. The low temperature part of the conductivity (a near temperature independent part, as in the case of present glass ceramics up to nearly 75 °C) can be explained on the basis of quantum mechanical tunneling model as suggested by Austin and Mott [39] with the procedure reported in a number of our earlier papers [40,41]. Based on quantum mechanical tunneling model, $N(E_F)$ is the density of the energy states near the Fermi level have been evaluated and values obtained are presented in Table 7. The value of $N(E_F)$ obtained $\approx 10^{20} \text{ eV}^{-1} \text{ cm}^{-3}$; such values of $N(E_F)$ suggest the localized states near the Fermi level are responsible for conduction. Further, the value of $N(E_F)$ is found to increase gradually from the sample N₂ to sample N₈, indicating an increase in the degree of disorder in the glass network.

Recollecting once again the observations on optical absorption and magnetic properties, and even dielectric studies reveal that the ratio Ni²⁺ (oct)/Ni²⁺ (tet) increases with increasing concentration of NiO crystallizing agent up to 0.8 mol% in the PbO–Sb₂O₃–As₂O₃ glass ceramics; further, the d–d transitions of the tetrahedral complexes are electric dipole allowed whereas those of octahedral complexes are electric dipole forbidden and are mainly due to the static or dynamic distortions from the regular octahedral geometry of the glass network and they can also be magnetic dipole allowed. As was reported by a number of other researchers [1], it is the octahedrally positioned Ni²⁺ ion that is responsible for the important luminescence emission transition ³T₂(F) → ³A₂(F) that peaks around 1280 nm; although we could not record the luminescence emission in the NIR range for lack of facility, the high intensity of octahedral optical absorption bands including ³A₂(F) → ³T₂(F) and

the results of the magnetic moments clearly indicate the possibility of high luminescence emission in glass ceramic sample N₈.

5. Conclusions

40PbO–(20–x)Sb₂O₃–40As₂O₃ glasses were crystallized with different concentrations (x = 0–1.5 mol%) of NiO. The XRD, SEM and DTA studies have indicated the presence of different crystalline phases in these samples. The studies on optical absorption and magnetic properties have indicated that there is a higher concentration of nickel ions that occupy tetrahedral positions in the samples crystallized with more than 0.8 mol% of NiO. The dielectric studies have indicated the growing degree of disorder in the glass network with increase in the concentration of crystallizing agent NiO up to 0.8 mol%; from these results it is concluded that within the concentration range of 0.2–0.8 mol%, the nickel ions mostly occupy octahedral positions and induce bonding defects causing the enhancement of the values of dielectric parameters. Finally, from the careful analysis of these results, it is felt that there is a possibility for getting high intense lasing emission (corresponding to ³A₂(F) → ³T₂(F) transition in the NIR region) if these glasses are crystallized with about 0.8 mol% of NiO.

Acknowledgements

This work is supported by Defence Research and Development Organization, Government of India in the form of Major Research Project (Grant No.: ERIP/ER/0503545M/01/946). The authors wish to thank Dr. Y.V. Swamy of IICT, Hyderabad for his help in thermal analysis of the samples and Mr N. Venkatramaiah of Pondicherry University for his help in taking SEM pictures of the samples used in the present study.

References

- [1] B. Wu, N. Jiang, S. Zhou, D. Chen, C. Zhu, J. Qiu, *Opt. Mater.* 30 (2008) 1900.
- [2] A.M. Malyarevich, Yu.V. Volk, K.V. Yumashev, V.K. Pavlovskii, S.S. zapalov, O.S. Dymshits, A.A. Zhilin, *J. Non-Cryst. Solids* 351 (2005) 3551.
- [3] M. Srinivasa Reddy, S.V.G.V.A. Prasad, N. Veeraiah, *Phys. Status Solidi (a)* 204 (2007) 816.
- [4] B.V. Raghavaiah, C. Laxmikanth, N. Veeraiah, *Opt. Commun.* 235 (2004) 341.
- [5] P.C. DeRose, M.V. Smith, K.D. Mielenz, D.H. Blackburn, G.W. Kramer, *J. Lumin.* 129 (2009) 349.
- [6] H. Keppler, N. Bagdasarov, *Chem. Geol.* 158 (1999) 105.
- [7] E. Zannoni, E. Cavalli, M. Bettinelli, *J. Phys. Chem. Solids* 67 (2006) 789.
- [8] S. Wang, K. Liang, *J. Non-Cryst. Solids* 354 (2008) 1522.
- [9] G. Murali Krishna, Y. Gandhi, N. Veeraiah, *Phys. Status Solidi (a)* 205 (2008) 177.
- [10] T. Suzuki, Y. Arai, Y. Ohishi, *J. Lumin.* 128 (2008) 603.
- [11] A. Jouini, A. Yoshikawa, Y. Guyot, A. Brenier, T. Fukuda, G. Boulon, *Opt. Mater.* 30 (2007) 47.
- [12] I.V. Kityk, *J. Phys. Chem. B* 107 (2003) 10083.
- [13] B. Zhang, Q. Chen, L. Song, H. Li, F. Hou, J. Zhang, *J. Non-Cryst. Solids* 354 (2008) 1948.
- [14] Y. Gandhi, K.S.V. Sudhakar, M. Nagarjuna, N. Veeraiah, *J. Alloys Compd.* (2009), doi:10.1016/j.jallcom.2009.06.115.
- [15] M. Nalin, M. Poulain, M. Poulain, J.L.R. Sidney, Y. Messaddeq, *J. Non-Cryst. Solids* 284 (2001) 110.
- [16] J.S. Wang, E.M. Vogel, E. Snitzer, *Opt. Mater.* 3 (1994) 187.
- [17] T. Satyanarayana, I.V. Kityk, M. Piasecki, P. Bragieli, M.G. Brik, Y. Gandhi, N. Veeraiah, *J. Phys. Condens. Matter* 21 (2009) 245104.
- [18] T. Satyanarayana, I.V. Kityk, K. Ozga, M. Piasecki, P. Bragieli, M.G. Brik, V. Ravi Kumar, A.H. Reshak, N. Veeraiah, *J. Alloys Compd.* 482 (2009) 283.
- [19] K. Nassau, *Bell Syst. Tech. J.* 60 (1981) 327.
- [20] A. Bishay, C. Maghrabi, *Phys. Chem. Glasses* 10 (1969) 1.
- [21] Y. Gandhi, N. Venkatramaiah, V. Ravi Kumar, N. Veeraiah, *Physica B* 404 (2009) 1450.
- [22] M. Nagarjuna, T. Satyanarayana, Y. Gandhi, N. Veeraiah, *J. Alloys Compd.* 479 (2009) 549.
- [23] L. Srinivasa Rao, M. Srinivasa Reddy, D. Krishna Rao, N. Veeraiah, *Solid State Sci.* 11 (2009) 578.
- [24] Powder Diffraction File, Alphabetical Index, Inorganic Compounds, JCPDS–International Centre for Diffraction Data, Newtown Square, PA, 2003, pp. 3273–19073.
- [25] P. Subbalakshmi, P.S. Sastry, N. Veeraiah, *Phys. Chem. Glasses* 42 (2001) 307.
- [26] B. Dubois, J.J. Videau, J. Portier, *J. Non-Cryst. Solids* 88 (1986) 355.
- [27] P.J. Miller, C.A. Cody, *Spectrochim. Acta A* 38 (1982) 555.
- [28] B.V. Raghavaiah, N. Veeraiah, *Phys. Status Solidi (a)* 199 (2003) 389.
- [29] J.J. Kleperis, P.D. Cikmach, A.R. Lulis, *Phys. Status Solidi (a)* 83 (1984) 291.
- [30] Y.R. Zakis, A.R. Lulis, Y.R. Lagzduns, *J. Non-Cryst. Solids* 47 (1982) 267.
- [31] D. Holland, *Solid State NMR* 26 (2004) 72.
- [32] A. Marotta, A. Buri, F. Branda, *J. Mater. Sci.* 16 (1981) 341.
- [33] E. Zannoni, G. Cavalli, M. Bettinelli, *J. Phys. Chem. Solids* 60 (1999) 449.
- [34] J.L. Rao, G.L. Narendra, S.V.J. Lakshman, *Polyhedron* 9 (1990) 1475.
- [35] J.D. Lee, *Concise Inorganic Chemistry*, fifth ed., Blackwell Science Ltd., 1996.
- [36] M. Nagarjuna, T. Satyanarayana, V. Ravi Kumar, N. Veeraiah, *Phys. B: Condens. Matter*, doi:10.1016/j.physb.2009.06.123.
- [37] A. Padmanabham, T. Satyanarayana, Y. Gandhi, N. Veeraiah, *Phys. Status Solidi (a)*, doi:10.1002/pssa.200925191.
- [38] S.V.G.V.A. Prasad, M. Srinivasa Reddy, N. Veeraiah, *J. Phys. Chem. Solids* 67 (2006) 2478.
- [39] G. Austin, N.F. Mott, *Adv. Phys.* 18 (1969) 657.
- [40] K. Sambasiva Rao, M. Srinivasa Reddy, V. Ravi Kumar, N. Veeraiah, *Mater. Chem. Phys.* 111 (2008) 283.
- [41] P. Venkateswara Rao, T. Satyanarayana, M. Srinivasa Reddy, Y. Gandhi, N. Veeraiah, *Physica B* 403 (2008) 3751.